Continuous synthesis of high-performance isobutylaluminoxanes in a compact and integrated approach

Yirong Feng, Mengbo Zhang, Haomiao Zhang*, Jingdai Wang, Yongrong Yang

State Key Laboratory of Chemical Engineering, College of Chemical and Biological Engineering, Zhejiang University, Hangzhou 310027, PR China

*Corresponding author. E-mail address: haomiaozhang@zju.edu.cn

Abstract

We present a 3D-printed continuous flow platform for controllable synthesis of isobutylaluminoxanes (IBAO), an effective olefin polymerization co-catalyst, via highly exothermic hydrolytic reaction of triisobutylaluminum (TIBA). This platform encompasses modules of mixing and reaction, in-line separation, and *in situ* UV-vis characterization. In addition, two NMR protocols are established to validate the results of in-line UV-vis analysis (^{31}P NMR) and reveal product structures (^{1}H NMR). Measured temperature profiles over the reactor indicate essentially fast heat removal, ensuring inherent safety. Subsequently, co-catalytic activity of IBAO is obtained by ethylene oligomerization experiments using an iron-based catalyst system at atmospheric pressure. Furthermore, we investigate the influence of key operating parameters including initial molar ratio between water and TIBA, initial TIBA concentration, and residence time. High IBAO yield over 98% and superior co-catalytic activity of ~5000 kg·(mol Fe)$^{-1}$·h^{-1} are achieved with optimized parameters in this single-pass platform, demonstrating the advantages of process.

KEYWORDS

continuous flow chemistry, 3D printing, multiphase reaction, in-line analysis, polymerization

1 INTRODUCTION

Alkylaluminoxanes are widely used activators in homogeneous polymerization and copolymerization of olefins in conjunction with metallocene compounds and multidentate late transition metal complexes such as compounds with Group IVB elements of titanium, zirconium, and hafnium.[1,2] In order to achieve high activity, alkylaluminoxanes are typically employed in significant excess amount with respect to the catalytic precursors (i.e. 10^3 – 10^4 mol/mol).[3-5] Among alkylaluminoxanes, methylaluminoxane (MAO) is the most popular for its highest co-catalytic activity in olefin polymerization; however, this benefit is accompanied by central challenges when synthesizing and handling MAO.[6-8] MAO is produced by hydrolysis of trimethylaluminum (TMA), while TMA is pyrophoric and thus handling TMA hydrolysis safely remains challenging even in laboratory scale. Moreover, this reaction is difficult to control with inevitable by-products (aluminum hydroxide) formation, resulting in a low MAO yield usually below 60% in multi-pass industrial process.[9-11] Pure MAO, commonly stored in aromatic solvents (i.e. toluene), is a white amorphous solid, and MAO solution is opaque, relatively viscous, and easily forms gels during sample aging due to intermolecular association.[12] MAO has low solubility and stability in aliphatic solvents, which further limits its applications.[13]

Based on the above concerns, modified methylaluminoxanes (MMAOs) that incorporate higher alkyl groups than methyl become an attractive alternative to MAO for their improved stability during storage, good solubility in aliphatic solvents,

reduced cost, and promising co-catalytic activity.[14,15] Isobutylaluminoxane (IBAO) is of practical interest as used in MMAOs components; in particular, IBAO exhibits high co-catalytic activity while employed alone in olefin polymerization.[16] Regardless of the difficulties in synthesis, it would be economically advantageous to replace the expensive MAO product with IBAO. Consequently, it deserves devoting additional efforts to find out a better synthetic approach to make high-performance IBAO, verify its activity, and compare with MAO.

IBAO is usually synthesized by partial hydrolysis of triisobutylaluminum (TIBA or $i-Bu_3Al$) with free water, as presented in Scheme 1 (Eqs. 1-5).[17-19] Other than free-water approach, IBAO was reportedly synthesized using ice or copper sulfate pentahydrate ($CuSO_4 \cdot 5H_2O$) as water source, and showed good co-catalytic activity when used with dimethylated zirconocene complexes in propylene polymerization.[16,20] Similar to MAO synthesis, IBAO is produced through batch or semi-batch operations in general, which are faced with several major bottlenecks: a) long reaction time and aluminum loss with hydrated salts as water source, b) high risks of runaway reactions and even explosions, c) low-temperature requirement for safety, d) poor batch-to-batch reproducibility, and e) the use of unusual or complicated reactors.

SCHEME 1 Formation of tetra-, oligo-, and poly-IBAO via TIBA hydrolysis.

$$i-Bu_3Al + H_2O \rightarrow i-Bu_3Al \cdot OH_2 \quad (1)$$

$$i-Bu_3Al\cdot OH_2 \rightarrow i-Bu_2AlOH+i-BuH \quad (2)$$

$$i-Bu_2AlOH+i-Bu_3Al \rightarrow i-Bu_2Al-O-i-Bu_2Al+i-BuH \quad (3)$$

$$n\,i-Bu_2AlOH \rightarrow \left[i-Bu_2Al(\mu-OH)\right]_n \quad (4)$$

$$\left[i-Bu_2Al(\mu-OH)\right]_n \rightarrow \left[i-BuAlO\right]_n+n\,i-BuH \quad (5)$$

An avenue to overcoming above obstacles is to use microreaction technique and continuous flow chemistry. Different from conventional batch processes, such novel approach has played an important role in synthesis of specialty chemicals, polymers, and nanomaterials, and thus encompassed a wide array of commercial equipment and applications.[21-25] In particular, modular and customizable flow chemistry platforms allow for rapid screening of reaction parameters, reaction optimization, handling of hazardous chemicals or explosive reactions, and scalable production.[26] End-to-end process design of chemicals in a compact reconfigurable system enables on-demand manufacturing units based on reactors, separators, and in-line characterization tools.[27,28] Moreover, leveraging 3D printing to manufacture mixers, reactors, and connectors in flow chemistry opens new design freedom and rapidly creates complicated structures that are difficult to make using conventional subtractive manufacturing processes in a whole piece.[29-32] The use of 3D printing further allows researchers to control and simply iterate the geometric parameters of

reactors to direct chemical synthesis toward the best performance.[33-35]

Based on the aforementioned advantages, we propose a new synthetic approach to make IBAO via TIBA hydrolysis, by combining the concepts of flow chemistry and 3D printing and achieving mixing, reaction, separation, and in-line analysis in modular designs. Specifically, the mixing module generates microdroplets of water to improve IBAO selectivity with enhanced biphasic mass transfer; the reaction module handles the fast and exothermic hydrolytic reaction of TIBA in a well-controlled manner and facilitates manipulation of reaction performance; the following in-line separation module removes gas product from liquid streams continuously and avoids any influence of bubbles on subsequent analysis; the *in situ* characterization module allows for continuous monitoring of reaction progress and a better understanding of nondestructive unit operations. Furthermore, two NMR (nuclear magnetic resonance) protocols are developed to verify the in-line UV-vis analysis results (via ^{31}P NMR) and reveal product structures (via ^{1}H NMR). Then we investigate the effects of main operating parameters (i.e. reagent concentration, initial molar ratio of water and TIBA, and residence time) on conversion of TIBA, yield of IBAO, and co-catalytic activity of the product.

2 MATERIALS AND METHOD

2.1 Materials

Toluene (99.5%), triphenylphosphine (PPh_3, 99%), ethylene diamine tetraacetic acid (EDTA), hexamethylenetetramine (99%), phosphoric acid (85 wt.% in water), and zinc sulfate heptahydrate ($ZnSO_4$, 99.5%) was obtained from Aladdin Bio-Chemistry Co. (Shanghai, China). Triisobutylaluminium (TIBA, 1.0 mol/L in toluene) and toluene-d_8 was purchased from Macklin Biochemical Co. (Shanghai, China). Chemicals including iron acetylacetonate ($Fe(acac)_3$, 99%), 2,6-diacetylpyridine (97%), and 4-methoxy-2-methylaniline (98%) were purchased from J&K Chemical Co. (Shanghai, China). Tungsten(VI) oxychloride ($WOCl_4$, 98%) was purchased from Sigma-Aldrich (USA). 10 wt.% MAO (methylaluminoxane) and TMA (trimethylaluminum) in toluene was purchased from Albemarle Corporation (Baton Rouge, LA, USA). All chemicals were used as received. All manipulations of air- and moisture-sensitive compounds were carried out under nitrogen atmosphere using standard Schlenk techniques or in a nitrogen glove box. Prior to experiments, toluene was dried over 4 Å molecular sieves, and further treated by a solvent purification system (PS-400-5-SD, Innovative Technology, USA), distilled deionized water was degassed by freeze-pump-thaw cycling, and TIBA was diluted in toluene for the required concentration. High purity nitrogen (99.999%) and polymerization-grade ethylene (99.9%) was both obtained from SINOPEC (Shanghai, China) and passed through oxygen- and moisture-scrubbing columns prior to use.

2.2 Flow platform

Figure 1 illustrates a laboratory-scale continuous flow system for the synthesis of IBAO by controlling the blend of small amount of water in toluene and TIBA/toluene. This platform consists of three syringe pumps to deliver reagents, a mixing and reaction module assisted by a high-speed camera and a thermal imaging camera, a gas-liquid separator, and an *in situ* characterization module. Except for the separator and the following three-way valve, all functional devices are fabricated using a commercial Form 2 SLA 3D printer (Formlabs, MA, USA) with a clear resin (FLGPCL04) of sufficient chemical compatibility.

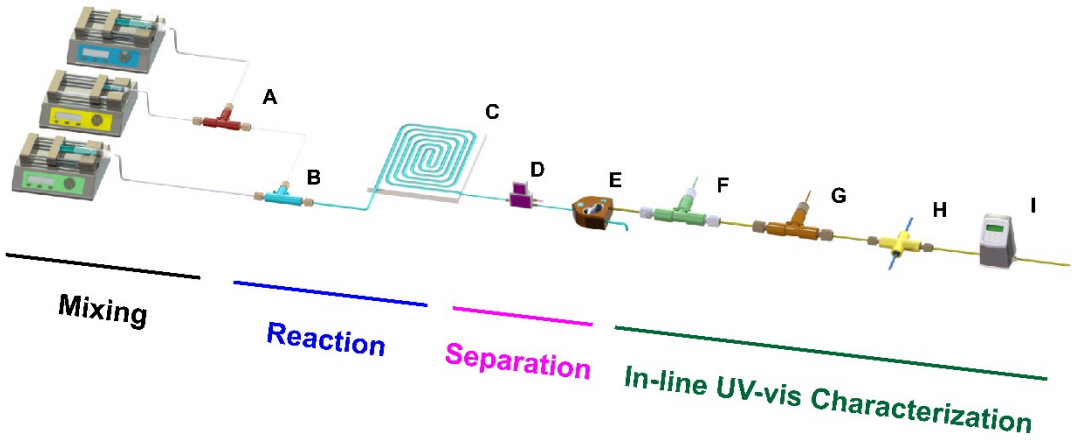

FIGURE 1 Illustration of the continuous flow platform for IBAO synthesis with three pumps (blue: water; yellow: toluene; green: TIBA/toluene), a microdroplet generator (A), a T-microreactor (B), a PFA tubular reactor embedded in a plastic substrate (C), a gas-liquid separator (D), a three-way valve (E), a second T-micromixer (F), a third T-micromixer (G), a flow cell for Ultraviolet (UV)–vis analysis (H), and a volumetric flowmeter (I).

2.2.1 Mixing and reaction

The mixing and reaction module encompasses a customized microdroplet generator (Figure 2a), a T-shape microreactor (Figure 2b), and a tubular reactor (Figure 2c) made by PFA (perfluoroalkoxy alkanes). In order to safely handle and control the violent hydrolytic reaction of TIBA and enhance mass transfer, we design and assemble a microdroplet generator that can produce small water droplets (Figure 2a), whereby a capillary tube with inner diameter (I.D.) of 0.1 mm and outer diameter (O.D.) of 0.16 mm is inserted into a 3D-printed T-junction via nuts and ferrules. The other end of the capillary tube is secured in a PFA tubing (I.D. 0.25 mm). By design, water flows through the capillary in the center of the tubing, while toluene circulates within the PFA tubing outside the capillary. Growing water dripping in the capillary orifice enables the detachment to generate monodisperse microdroplets when the forces exerted by the co-flowing continuous phase (toluene) exceed the surface tension. This simple and efficient fabrication method offers advantages over conventional microdevices manufacturing that is usually tedious and expensive.

In the next, the water droplets travel with toluene through the PFA tubing (I.D. 0.25 mm) and then mix with the TIBA/toluene solution at the confluence of a 3D-printed T-microreactor (Figure 2b). This microreactor, with an inner diameter of 3.0 mm, offers first-stage reagents blending. The small reactor size limits the extremely fast and exothermic TIBA hydrolysis to a low volume to mitigate risks of a thermal runaway. To ensure enough residence time, the reactive flow goes through a 1.12 m long PFA tubing (I.D. 1.59 mm), which is placed inside a compact, 3D-printed substrate (Figure 2c). This substrate is made by plastic resin with significantly lower heat conductivity

than metals/alloys, as a thermal barrier to reduce interactions of heat exchange between the hot zone and its neighboring cold zone. In parallel, such design allows for imaging studies via a high-speed camera and a thermal camera, to help understand the reaction progress and heat removal capability. More importantly, we design this platform to handle the highly exothermic reaction at room temperature (20 °C), instead of the conventional processes to produce aluminoxanes usually at -78 °C[11] for safety.

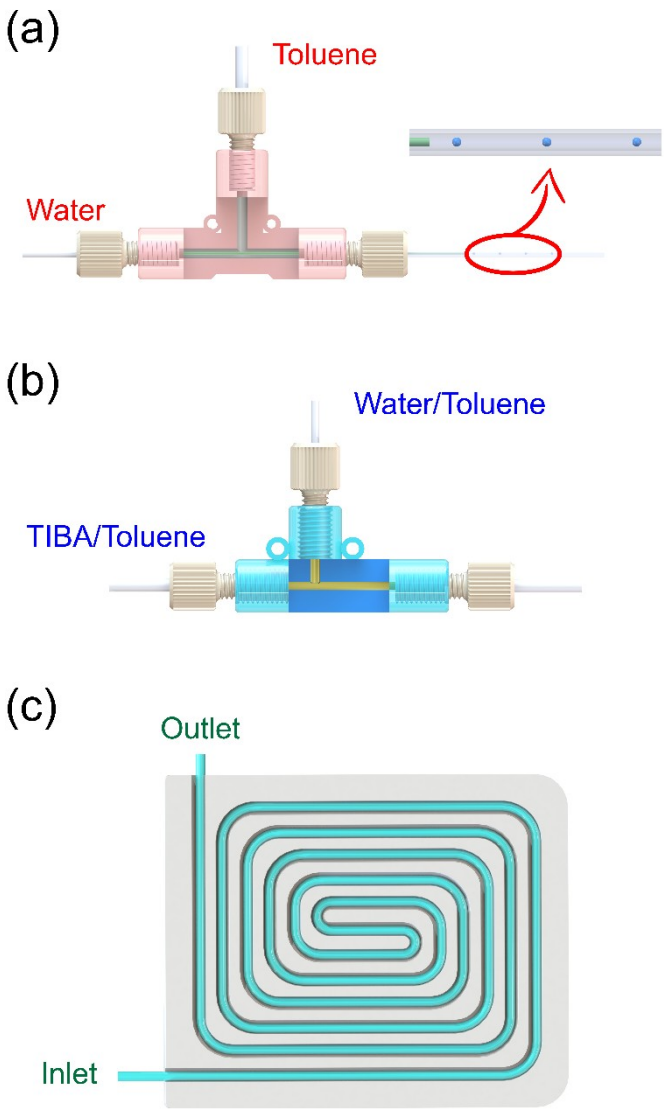

FIGURE 2 3D-printed key functional devices designed for mixing and reaction, including (a) a microdroplet generator, (b) a T-microreactor, and (c) a PFA tubular reactor.

To evaluate thermal management and prevent runaway reactions, we further fit and find the effective heat transfer coefficient (h in $W/(m^2 \cdot K)$) using experimental data and a MATLAB algorithm. The governing equation is described in Eq. 6, as a version of the Graetz problem of steady-state diffusion-controlled transport from a surface into a tubular laminar flow.[36]

$$U_{max}\left[1-\left(\frac{r}{R}\right)^2\right]\frac{\partial T}{\partial z}=\alpha\left[\frac{1}{r}\frac{\partial}{\partial r}\left(r\frac{\partial T}{\partial r}\right)\right] \quad (6)$$

Here, U_{max} is the maximum velocity existing at the centerline in m/s, T is the temperature in K, R is the radius 0.794 mm, $\alpha = k/\rho C_p$ is the thermal diffusivity of the fluid, C_p is the heat capacity at constant pressure of the fluid in $J/(kg \cdot K)$, and k is the thermal conductivity of the fluid in $W/(m \cdot K)$. As the concentration of all species is very diluted, we take the material properties (i.e. $C_p(T)$'$k(T)$) of pure toluene for calculation. The corresponding boundary conditions used are (i) inflow temperature (T_0 is the measured inlet temperature in K), (ii) axis-symmetry, and (iii) convective heat flux at wall surface (Eq. 7, T_{ext} is the ambient temperature 293K).

$$-k\frac{\partial c}{\partial z}\bigg|_{wall}=h\cdot\left(T_{ext}-T\right)(7)$$

2.2.2 Reaction analysis

We use the following expressions (Eqs. 8-9) to determine the conversion of TIBA (X_{TIBA}) and the yield of IBAO product (Y_{IBAO}):

$X_{TIBA}=¿$

$$Y_{IBAO}=\frac{\dot{n}_{IBAO,out}}{\dot{n}_{TIBA,\in¿}\times 100\%}(9)¿$$

Here, $\dot{n}_{TIBA,\in¿¿}$ and $\dot{n}_{TIBA,out}$ are the molar flowrates of TIBA in the solution at the inlet and the outlet, respectively, and $\dot{n}_{IBAO,out}$ is the molar flowrate of IBAO at the outlet. To complete the calculation, we need to know $\dot{n}_{TIBA,out}$ and $\dot{n}_{IBAO,out}$.

We employ in-line UV-vis analysis to determine $\dot{n}_{TIBA,out}$, enabled by the complexation reaction between tungsten(VI) oxychloride ($WOCl_4$) and TIBA. The UV spectrum of $WOCl_4$ in toluene shows a distinct band with its maximum locating at a wavelength (λ) of 355 nm. Kinetic analysis of the reaction between $WOCl_4$ and TIBA indicates that TIBA forms a complex with $WOCl_4$ before it acts as an alkylating agent.[37] The resulting complex has the same absorbance spectrum as pure $WOCl_4$ but with a smaller absorption coefficient. Therefore, based on this knowledge, we design an *in situ* characterization module for essentially the first time, aided by a gas-liquid separator and two customized micromixers to remove isobutane and introduce

toluene and $WOCl_4$, respectively.

In order to monitor the fluids via in-line UV-vis, the tubular reactor outlet is connected to a membrane separator (Zaiput Flow Technologies, MA, USA) with a hydrophilic membrane for isobutane removal. In the meantime, a flow integrating instrument, connected with the gas outlet, collects and measures the volume of isobutane. The moles of isobutane are subsequently calculated using the ideal gas equation of state. The liquid stream then flows into a three-way valve, where one outlet is used to collect the product (IBAO/TIBA), and the other opens only when in-line UV-vis analysis is required. Such design ensures continuous UV-vis monitoring of the liquid stream, not interrupted by any gas bubbles.

After the three-way valve, toluene can be introduced through a customized T-micromixer (Mixer A, I.D. 3.0 mm) for dilution when the remaining TIBA concentration is over high. Then, $WOCl_4$ is added as an indicator via a pre-mixed $WOCl_4$/toluene solution and blended with the liquid stream at another T-micromixer (Mixer B, I.D. 3.0 mm) that is the same as Mixer A. Simultaneous mixing is presumably achieved in both T-micromixers for the smaller mixer dimensions and low flowrates. When implementing in-line UV-vis analysis, we note that a low volume is beneficial to keep the residence time distribution sharp, ensuring rapid equilibration of reagents. A customized flow cell (cross-connector) is designed, 3D printed, and adapted to secure a UV-transparent FEP (fluorinated ethylene propylene) tubing (I.D. 0.75 mm, O.D. 1.59 mm); perpendicular to the FEP tubing, two 400 μm optical fibers (QP400-

2-UV-VIS, Ocean Optics) connect the UV light source with a high-resolution spectrometer (FLAME-S-UV-VIS, Ocean Optics) to measure the absorbance of the reactive fluids. Meanwhile, the transient liquid flowrate through the flow cell is measured by a volumetric flowmeter.

In order to verify the newly developed in-line UV protocol, we further investigate an off-line characterization method with ^{31}P NMR to measure the TIBA concentration in the product sample which contains IBAO/toluene with a small amount of unreacted TIBA. This measurement is based on that aluminum trialkyls react rapidly and reversibly with PPh_3 to form a Lewis acid-base complex but do not react with IBAO. The rapid exchange of free PPh_3 and TIBA-PPh_3 makes the ^{31}P NMR signal a weighted average, such that the amount of TIBA can be determined aided by an external standard (85 wt.% H_3PO_4 in water). Furthermore, ^{1}H NMR results obtained from IBAO product samples provide insights into the structure determination of IBAO.

In addition, we use a titration method to determine the concentration of aluminum element that consists of both TIBA and IBAO in the product sample. When little by-product is formed, the aluminum concentration in the product should be nearly identical to the initial concentration of TIBA. Finally, the molar amount of IBAO ($\dot{n}_{IBAO,out}$) is obtained by subtracting the amount of TIBA using the total molar amount of aluminum.

2.3 Experimental procedure for IBAO synthesis

In order to hook up the flow assembly, each fluidic port from all 3D-printed functional devices is tapped with an embedded screw thread (1/4”-28) and fluidic connection is enabled using IDEX 1/4”-28 fittings with PFA/FEP tubing with I.D. 1.59 mm and O.D. 3.18 mm. Smaller size PFA tubing (I.D. 0.25 mm and O.D. 1.59 mm) is employed to deliver water. Prior to experiments, the entire flow platform undergoes several cycles of vacuum and nitrogen blowing to remove any residual air. During experiments, the entire flow platform is kept at room temperature (20 ^{o}C).

For IBAO synthesis, reagents of water, toluene, and a pre-mixed TIBA/toluene solution are fed through three syringe pumps (Longer Precision Pump, LSP01-1A) for better process control. To form tiny water droplets in toluene, water is injected into the microdroplet generator at a flowrate range of 30 – 100 μL/min, while toluene is injected at a higher flowrate of 0.25 – 3.0 mL/min. In order to analyze the size and distribution of water droplets, we monitor and record the process of microdroplet generation in different flowrate pairs with a high-speed camera (Photron FASTCAM Mini WX100, Japan) in conjunction with a Nikon camera autofocus lens (AF 50/1.8D). An image processing program via ImageJ is employed to extract the feature of microbubbles, i.e. the Sauter mean diameter (d_{32}).[30] The TIBA/toluene solution is introduced at a flowrate of ≥6.0 mL/min with TIBA concentration ranging between 0.5 – 1.0 mol/L. To obtain optimized reaction performance, we manipulate the initial molar H_2O/TIBA in the range of 0.5 – 1.0 via adjustment of flowrates. In addition, we use the high-speed camera and thermal imaging camera (A655sc, FLIR, Sweden) to record the tubular reactor for reaction dynamics (i.e. gas

formation, trends of two-phase flow) as well as the temperature profiles along the reactor with a sampling frequency of 60 Hz.

Considering in-line UV-vis analysis, toluene is introduced from Mixer A and a pre-mixed $WOCl_4$/toluene solution is introduced through Mixer B to form $WOCl_4$-TIBA complex. In addition, we perform separately the reaction between $WOCl_4$ and TIBA in Mixer B to obtain a calibration line for quantitative analysis. Two syringe pumps are used to deliver TIBA/toluene solution with different TIBA concentrations and 4.0 mmol/L $WOCl_4$ in toluene with identical flowrates, respectively. Then, the mixed solution, with molar TIBA/$WOCl_4$ from 0 – 10, is monitored by the flow UV-vis spectrometer at a distance of 10 cm from Mixer B.

Regarding NMR analyses, we switch the valve position from in-line UV to product collection. With the IBAO/toluene sample, ^{1}H NMR spectra are obtained using a sealed NMR tube at 600 MHz on an Agilent DD2 (DirectDrive2) instrument. ^{1}H NMR data are recorded in toluene-d_8. The obtained ^{1}H NMR spectra are referenced to the signals of the residual methyl group in toluene (δ_H = 2.09 ppm). Moreover, the moles of unreacted TIBA in the sample are determined by ^{31}P NMR upon addition of excess PPh_3.[38]

During the titration analysis, a precisely weighed IBAO/toluene solution is added into a Schlenk flask and decomposed by slow injection of water. Then the acidity of this solution is adjusted to pH of 3.0 with aqueous sulfuric acid (10% v/v). A certain amount of EDTA is added, and then the solution is refluxed for 3 min. Subsequently,

hexamethylenetetramine (ca. 2.0 mg) is added until the pH reaches 6.0. The mixture is titrated with an aqueous $ZnSO_4$ solution (0.02 mol/L) using xylenol orange as an indicator (yellow-red).

2.4 Polymerization

We perform ethylene oligomerization experiments at atmospheric pressure using a homogeneous catalytic system composed of bis(imino)pyridine iron complexes (L-Fe(acac)$_3$) and IBAO (Scheme 2). Bis(imino)pyridine iron complexes exhibit excellent catalytic activity for linear alpha-olefins (α-olefins) production when used with aluminoxanes. In this catalyst system, iron acetylacetonate (Fe(acac)$_3$) is employed as the iron source to form a homogeneous pre-catalyst with a 2,6-bis[1-(4-methoxy-2-methylphenylimino)ethyl]pyridine ligand (L) that is synthesized by reaction between 4-methoxy-2-methylaniline and 2,6-diacetylpyridine, as shown in Scheme 3.

SCHEME 2 Ethylene oligomerization using L-Fe(acac)$_3$ and IBAO.

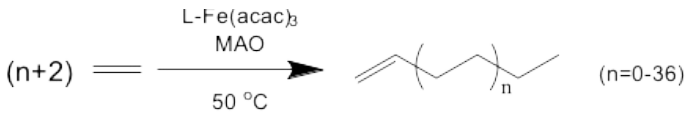

SCHEME 3 2,6-bis[1-(4-methoxy-2-methylphenylimino)ethyl]pyridine (L) synthesis.

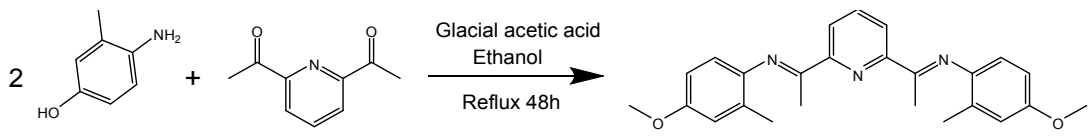

2.4.1 Preparation of Bis(imino)pyridine iron complexes

To prepare the catalyst, 4-methoxy-2-methylaniline is added to a solution of 2,6-diacetylpyridine in absolute ethanol. The solution is refluxed for 48 h after dropping a small amount of glacial acetic acid. Upon cooling to room temperature, the product is crystallized out from ethanol, and subsequently filtered, washed with cold ethanol, and dried in a vacuum oven at 60 °C overnight. Then, the bis(imino)pyridine ligand is mixed with $Fe(acac)_3$ in identical molar ratio and dissolved in toluene, forming a homogeneous orange-red mixture solution, abbreviated as L-$Fe(acac)_3$. Concentration of this catalyst precursor in toluene, in terms of iron atoms, is 4.0 μmol/mL.

2.4.2 Ethylene oligomerization experiment

Ethylene oligomerization experiments are performed in a 250 mL dried three-necked round-bottom flask that is immersed in a Magnetism Msier with an agitation speed of 800 rpm. A continuous and steady stream of ethylene is introduced into the flask under stirring. The desired amounts of toluene (50 mL), IBAO and L-$Fe(acac)_3$ (2.0 μmol) are added sequentially into the flask, in which the amount of IBAO is calculated based on a set molar Al/Fe of 1000. The addition of catalyst immediately initiates ethylene oligomerization, which lasts for 30 min at atmospheric pressure. Upon completion, the reaction is quenched by introducing an acidified ethanol solution, followed by the product being separated out via filtration. The insoluble polyethylene wax product is washed out and dried overnight at 60 °C under reduced pressure until a constant weight is achieved. For soluble oligomers, an internal

standard (n-heptane, 1.0 mL) is injected into the liquid phase, such that α-olefin products ranging from C_4 to C_{36} are quantitatively analyzed by gas chromatography (Agilent GC 6890 equipped with an Agilent HP-5 column). The yield of volatile C_4 fraction is determined by extrapolation based on the α value, as a characteristic coefficient of the Schulz-Flory distribution calculated using the relative rate between chain propagation and chain termination or the molar ratio of two subsequent oligomer fractions (C_{14} and C_{12} in this case). The co-catalytic activity is determined using the combination of the soluble oligomers and insoluble polymers products.

3 RESULTS AND DISCUSSION

3.1 Microdroplet formation

Monodisperse microdroplets of water are generated in the capillary-based device. Figure 3 illustrates the Sauter mean diameter of the formed droplets under water flowrate of 30 and 60 μL/min and toluene flowrate of 0.25 – 3.0 mL/min. The overall size distribution of droplets is from 150 to 400 μm while manipulating both the flowrates of water and toluene. Highly uniform droplets in size that are crucial to biphasic mass transfer are obtained for each flowrate with ±5% measurement error. As toluene flowrate exceeding 2.0 mL/min, the droplet size reaches a plateau, suggesting a suitable condition to handle reactions. Furthermore, we find that the flowrate of the disperse phase (water) has minor effect on the droplet size, implying that a wider range of water flowrate may be applied. Therefore, we start IBAO synthesis experiments with 160 – 180 μm water droplets at low flowrates of toluene

for improved reaction performance.

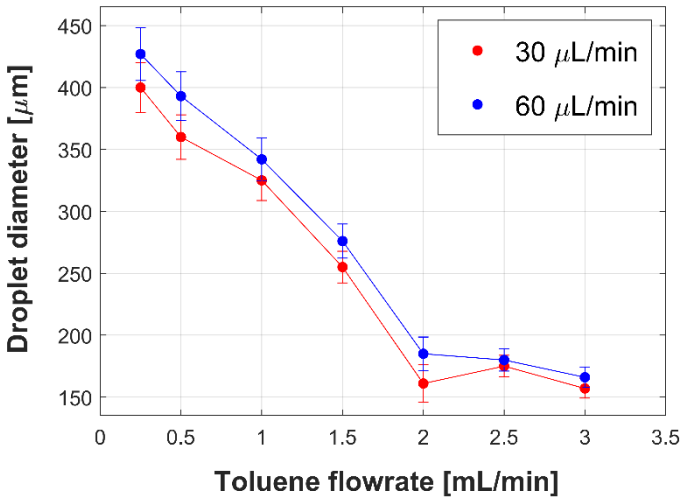

FIGURE 3 Performance of water microdroplet formation under water flowrate of 30 and 60 µL/min and toluene flowrate of 0.25 – 3.0 mL/min.

3.2 Tubular reactor performance

Figure 4a presents a typical image of reactor with volume of ~2.5 mL obtained from the high-speed camera during TIBA hydrolysis. As reaction proceeds, the generated isobutane continues to coalesce and thus forms gas slugs. Different from synthesis of MAO, no solid by-products are visible in the process, indicating high selectivity to IBAO. In parallel, the thermal imaging camera records the temperature evolution at steady state (Figure 4b). The hydrolytic reaction of TIBA is highly exothermic, as evidenced by the measured inlet flow temperature as high as 53.5 ℃. This temperature rise (33.5 ℃) occurs essentially in no time, even though only small amounts of reactants are consumed, demonstrating the advantages of using microreactors. Along the reactor, the low thermal conductivity of the 3D-printed

plastic plate and strong forced convection cools down the temperature effectively (outlet temperature reduces to 27.3 $℃$ at 1.12 m), mitigating risks of runaway reactions. Furthermore, the heat transfer coefficient ($_h$) is fitted to be 35.5 $W/(m^2 \cdot K)$, as shown in Figure 4c. Owing to the high area-to-volume ratio of microreactors, improved wall-to-fluid heat transfer rates become possible, which enable the use of more concentrated reactants while maintaining an inherent safe design. In addition, based on the above analysis, we shorten the reactor length to 0.47 m for following reaction study, given the fast kinetics and sufficient residence time, which might not affect the reaction performance.

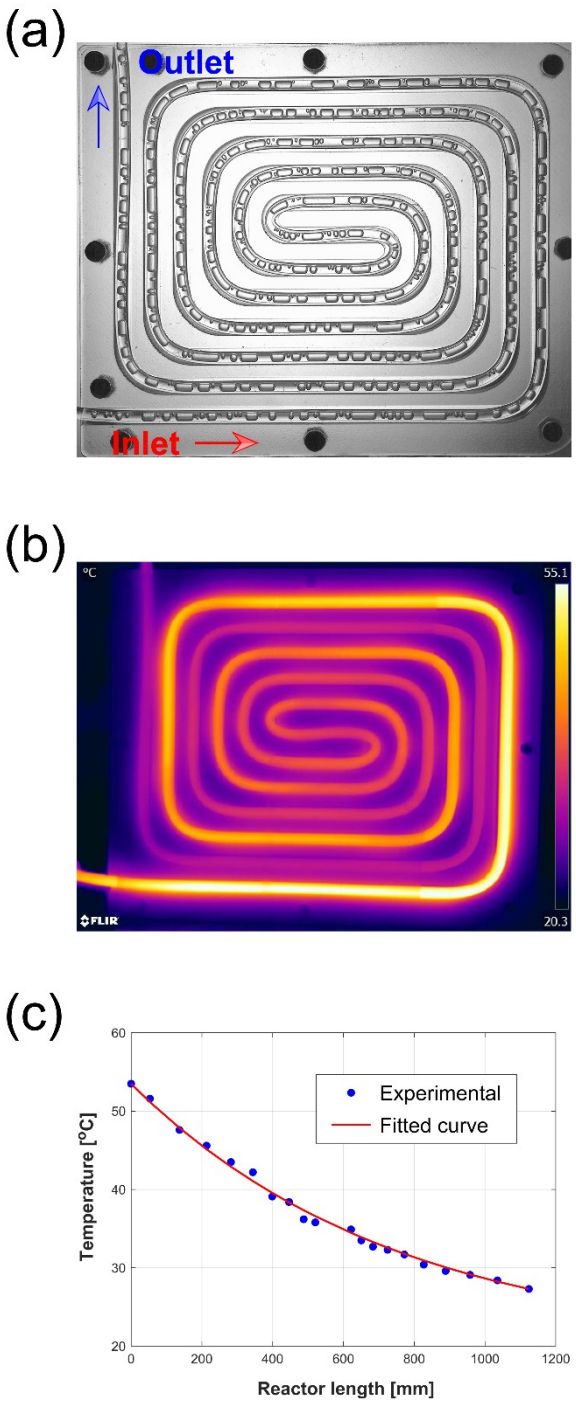

FIGURE 4 Typical images showing reaction progress obtained using (a) high-speed camera and (b) thermal camera, and (c) temperature profiles versus reactor length, under initial H_2O/Al of 0.75, TIBA initial concentration of 0.52 mol/L, and mean residence time of 18.9 s (water flowrate of 42 μL/min, toluene flowrate of 2.0 mL/min,

and TIBA/toluene flowrate of 6.0 mL/min).

3.3 In-line analysis

Figure 5a illustrates the UV-vis spectra of pure $WOCl_4$ and TIBA-$WOCl_4$ complex at TIBA concentration of 6.62 and 32.3 mmol/L, respectively. Pure $WOCl_4$ has the highest peak at 355 nm in the UV-vis spectra; the other two peaks are attributed to the formation of TIBA-$WOCl_4$ complex, in which higher TIBA concentration leads to greater reduction of peak. In order to obtain a calibration curve, we measure five samples with different TIBA concentration and plot the normalized absorbance ($\Delta A/A_0$) and molar TIBA/$WOCl_4$ ($\frac{n_{TIBA}}{n_{WOCl_4}}$) as indicated in Figure 5b, in which A_0 denotes the absorbance of pure $WOCl_4$ and ΔA is the difference between A_0 and absorbance of the TIBA-$WOCl_4$ complex, both at 355 nm. It clearly shows that, as $\frac{n_{TIBA}}{n_{WOCl_4}}$ increases, the normalized absorbance $\Delta A/A_0$ at 355 nm increases and a linear relationship is satisfied (Eq. 11) with a linear regression R^2 of 0.996.

$$\frac{\Delta A}{A_0} = 0.032 \times \frac{n_{TIBA}}{n_{WOCl_4}} + 0.233 \quad (11)$$

Therefore, TIBA concentration in the fluids can be determined using the calibration

line with good accuracy. In this particular case, such *in situ* characterization module inherently prevents any exposure of sensitive reagents to air or steam while monitoring TIBA without generating additional volume hold-up.

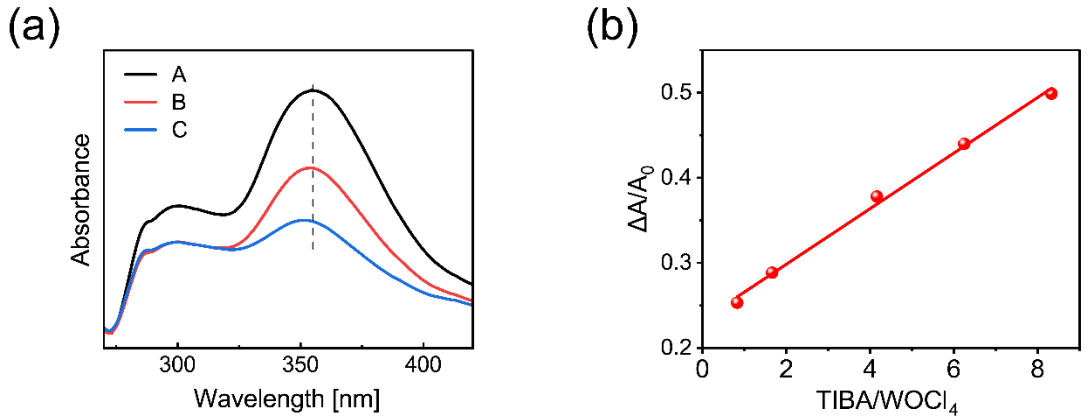

FIGURE 5 (a) The UV-vis spectra of pure $WOCl_4$ (A) and TIBA-$WOCl_4$ complex at two different TIBA concentrations (B: 6.62 mmol/L, C: 32.3 mmol/L). (b) The calibration line that correlates the normalized absorbance $\Delta A/A_0$ and molar TIBA/$WOCl_4$.

^{31}P NMR offers an alternative to quantify the amount of aluminum, thus being employed to validate the in-line UV-vis analysis. The ^{31}P NMR calibration result is plotted in Figure 6, in which chemical shifts are reported in ppm relative to the external standard H_3PO_4 (H_2O). This plot correlates linearly the elemental molar ratio

of aluminum and phosphorus ($\frac{n_{Al}}{n_P}$) with the chemical shift ($_{\delta}$) for a mixture of TIBA and PPh_3 in toluene-d_8, yielding a linear regression R^2 of 0.998 (Eq. 12). The TIBA concentration obtained with ^{31}P NMR matches well with that determined using in-line UV-vis, leading to a difference within ±8%. Therefore, the developed UV-vis protocol is capable of monitoring the transient reaction progress.

$$\frac{n_{Al}}{n_P} = -0.488 \cdot \delta - 2.27 \quad (12)$$

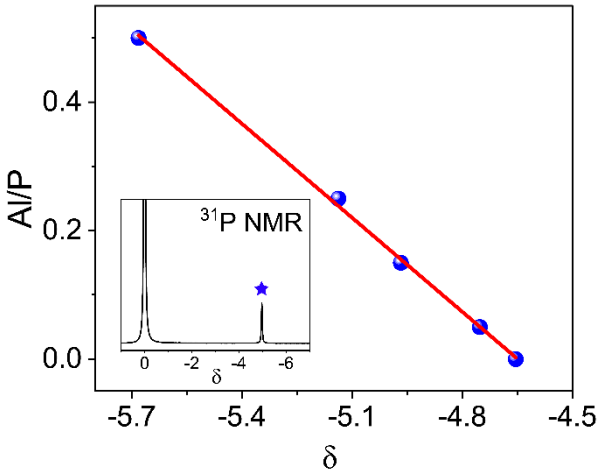

FIGURE 6 Linear correlation between molar Al/P and the ^{31}P NMR chemical shift for a mixture of TIBA and PPh_3 in toluene-d_8.

3.4 Reaction analysis and co-catalytic activity

3.4.1 Influence of H_2O/Al

The mass balance of aluminum and carbon both closes well (¿±5%) for all reactions, as indicated by the UV-vis, NMR, titration, and gas volume measurements. A key benefit of the flow approach is to run reactions at steady state ensuring enough process stability. A closer look at the steady-state reaction outcomes would reveal the importance of manipulation of key operating parameters. To this end, we investigate in the first place the initial molar ratio between water and TIBA (H_2O/Al) in the feed solution, as the most critical factor that influences significantly the reaction progress and the structures of IBAO product.

Figure 7a illustrates the comparison of ^{1}H NMR spectra of IBAO/toluene products obtained with different H_2O/Al. At H_2O/Al of 0.50 (blue curve of Figure 7a), the signals of methyl group and methylene group are presented by the superposition of broad, weakly resolved peaks from IBAO including δ ~1.2 (methyl) and doublet at δ ~0.5 (methylene), respectively, and small peaks from unreacted TIBA (δ ~1.1 and δ ~0.22). The big broadened peak from δ ~1.4 – 0.9 presumably indicates the exchange of the isobutyl groups between TIBA and IBAO, which illustrates the existence of TIBA/IBAO associates. The presence of TIBA may be explained by the formation of oligomeric aluminoxane products that consumes water. At H_2O/Al of 0.50, TIBA hydrolysis is preceded by Eqs. 1-2 and a further reaction between a hydroxy derivative and excess TIBA to afford tetraisobutylaluminoxane (tetra-IBAO, Eq. 3). As the relative amount of water further increases (i.e. H_2O/Al increases from 0.50 to 0.75 or 1.0), the doublet of methyl protons from TIBA at δ ~0.99 disappears, and the peak at δ ~1.1 becomes weaker than that at H_2O/Al of 0.50. This behavior

indicates the appearance of oligomeric and long-chain aluminoxane structures, corresponding to the formation of hydroxyl associates (Eq. 4) that gradually convert into a polymeric form of IBAO (poly-IBAO, Eq. 5).

Figure 7b illustrates the reaction performance in terms of TIBA conversion and IBAO yield under different H_2O/Al, as well as the co-catalytic activity of the as-synthesized IBAO. TIBA conversion and IBAO yield both increase as H_2O/Al increasing from 0.50 to 0.75; however, when this ratio further increases to 1.0, the improvement of conversion is very small, and the yield is maintained at ~91%. This result further confirms that at small H_2O/Al, by-product formation remains minimal, and the selectivity to IBAO is close to 1.0. On the other hand, when H_2O/Al is 1.0, IBAO selectivity drops slightly. Therefore, we recommend H_2O/Al of 0.75 for further reaction analysis. Regarding all the syntheses of TIBA with various H_2O/Al, there are no visible solids captured by the high-speed camera, indicating that the risks of reactor clogging are largely mitigated using water microdroplets as reagent source.

Ethylene oligomerization experiments show that high co-catalytic activity is achieved with IBAO and bis(imino)pyridine iron complexes as catalysts when IBAO is synthesized at H_2O/Al of 0.75 and 1.0. Notably, the activity value exceeds 4000 kg·(mol Fe)$^{-1}$·h^{-1} at H_2O/Al of 0.75. At H_2O/Al of 0.50, the predominant formation of IBAO dimers $\left(i-Bu_2Al-\mu-O-i-Bu_2Al\right)_2$ may lead to the reduced co-catalytic activity.

For comparison, we also take a commercial MAO sample (Albemarle Corporation,

USA) as activator for the same polymerization study and obtain a co-catalytic activity of 3250 kg·(mol Fe)$^{-1}$·h^{-1} at H_2O/Al of 0.75. Therefore, it is evident that the as-synthesized IBAO is a powerful activator when used with an iron-catalyst in ethylene oligomerization.

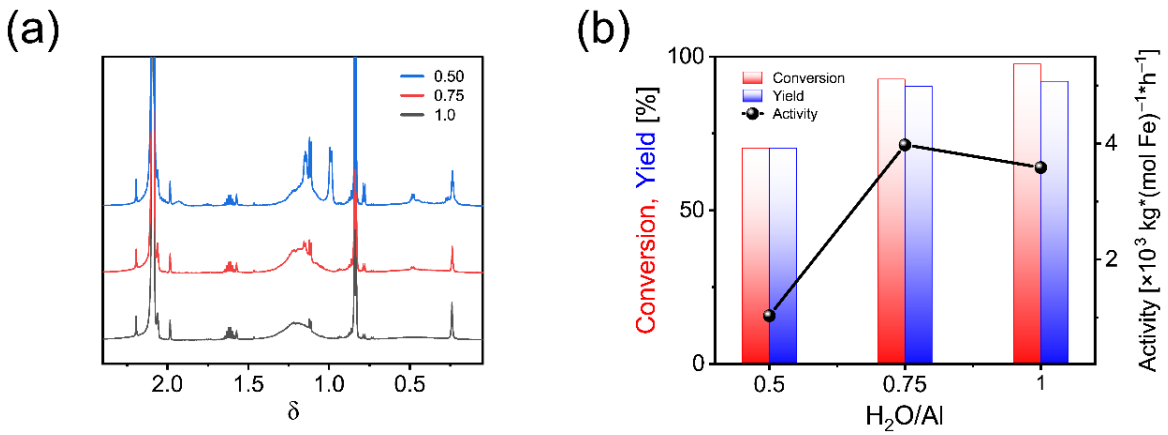

FIGURE 7 (a) ^{1}H NMR spectra of IBAO/toluene solution as synthesized under three different H_2O/Al (i.e. 0.50, 0.75, 1.0), and (b) influence of initial H_2O/Al on the reaction and co-catalytic performance, including TIBA conversion, IBAO yield and activity, all of which are obtained at TIBA concentration of 0.52 mol/L and mean residence time of 6.68 s.

3.4.2 Influence of TIBA concentration and residence time

Likewise, high feed concentration and short residence time are of great importance to large-scale production capability, especially when handling extremely fast reactions. To this end, we further explore the reaction at different TIBA concentration (Figure 8a-b) and at different residence time (Figure 8c-d) for reaction conditions

optimization while keeping H_2O/Al at the recommended value of 0.75. Figure 8a indicates that when TIBA concentration increases, IBAO concentration in the product sample increases proportionally with minimal unreacted TIBA remaining, as shown in the ^{1}H NMR spectra. In addition, both the IBAO yield and the corresponding co-catalytic activity for olefin oligomerization remain at similar levels, suggesting sufficient process stability (Figure 8b). Since this process is insensitive to an increase in TIBA concentration, therefore it is possible to scale the production with such manner.

Given that TIBA hydrolysis is extremely fast, decreasing residence time by increasing flowrate of the TIBA/toluene stream may be beneficial to larger production rate without sacrificing IBAO yield and activity. As demonstrated earlier, water flowrate influences insignificantly on the formed microdroplet size; therefore, at fixed H_2O/Al of 0.75 and TIBA concentration of 0.52 mol/L, flowrates of water and TIBA/toluene are increased proportionally to maintain reaction performance. The ^{1}H NMR spectra (Figure 8c) indicate that with a decrease of residence time, signal intensity of methyl group from TIBA becomes weaker, suggesting less TIBA remaining in the product sample. In addition, Figure 8d illustrates that both the TIBA conversion and IBAO yield exceed ~98% with an IBAO selectivity close to 100% when decreasing the residence time to 3.34 s or 4.45 s. In particular, the IBAO product exhibits the highest co-catalytic activity of ~5000 kg·(mol Fe)$^{-1}$·h^{-1} at mean residence time of 4.45 s, making it a desirable reaction condition for better production rate as well as activity. Under mean residence time of 3.34 s, the as-

developed single-pass flow platform is capable of producing 10.5 mol IBAO per day, assuming a molecular weight of 100 g/mol ($i-Bu-Al-O$). This production rate corresponds to four tons of 10 wt.% IBAO in toluene solution annually, which is high-throughput and potentially scaled out using multiple reactor components. Furthermore, the integrated synthetic approach is readily extended to produce other alkylaluminoxanes.

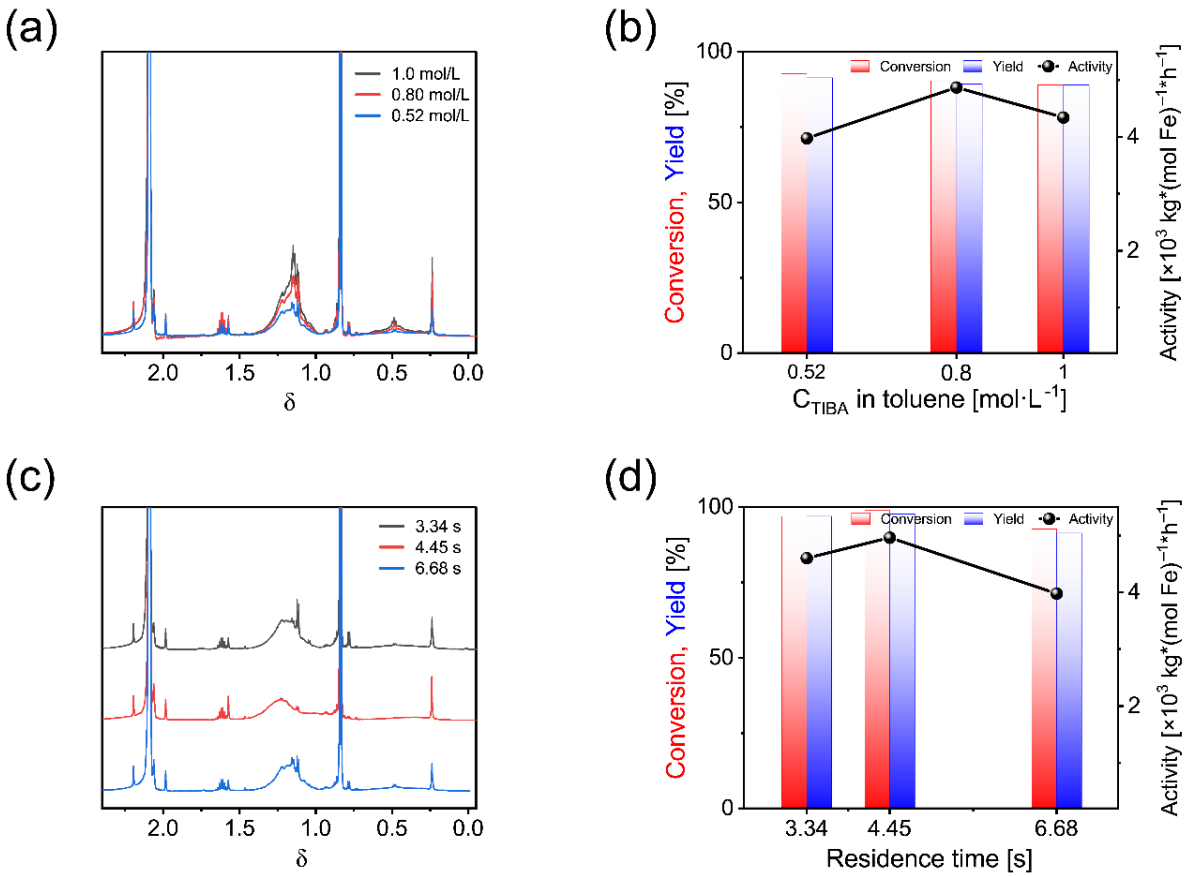

FIGURE 8 (a) ^{1}H NMR spectra of IBAO/toluene solution as synthesized under different TIBA concentration, and (b) effect of TIBA concentration on the reaction and co-catalytic performance, including conversion, yield and activity. Both (a-b) are obtained at H_2O/Al of 0.75 and mean residence time of 6.68 s. (c) ^{1}H NMR spectra of

IBAO/toluene solution as synthesized under different residence time, and (d) effect of residence time on the reaction and co-catalytic performance. Both (c-d) are obtained at H_2O/Al of 0.75 and TIBA concentration of 0.52 mol/L.

4 CONCLUSION

We develop a flow platform enabling IBAO synthesis with high throughput of 10.5 mol/day and high IBAO yield over 98% using optimized reaction conditions. To handle the extremely fast and exothermic hydrolytic reaction, we propose a low-volume approach with microreaction features that ensures inherent safety and precise control of reaction progress. The capillary-based microdroplet generator associated with tubular microreactor is proved to be efficient and effective during use. Temperature imaging measurement confirms the sufficient capacity to remove heat and prevent a thermal runaway, even when performing the reaction at room temperature. Moreover, the integrated reaction analysis tool via *in situ* UV-vis provides a rapid quantification of TIBA concentration and conversion. We also emphasize effects of the initial molar ratio of water and TIBA and find that this parameter, with a recommended value of 0.75, influences significantly the reaction progress as suggested by UV-vis and ^{31}P NMR and product structure revealed by ^{1}H NMR. In parallel, we demonstrate that the use of high feed concentration and short residence time, whenever applicable, offers a good choice to enhance production capability. Very importantly, the IBAO product exhibits superior co-catalytic activity in ethylene oligomerization experiments with an iron-based catalyst system, as

compared with a commercially available MAO sample for the same test. This lab-scale platform is readily extended to continuous synthesis of other alkylaluminoxanes, and presumably scaled out using multiple reactors.

ACKNOWLEDGMENTS

We thank the National Natural Science Foundation of China (21908190), the State Key Laboratory of Chemical Engineering of China (SKL-ChE-19T05), and the Fundamental Research Funds for the Central Universities of China (2019QNA4045) for financial support.

AUTHOR CONTRIBUTIONS

Yirong Feng: Conceptualization; data curation; formal analysis; investigation; methodology; resources; software; visualization; writing-original draft. **Mengbo Zhang**: Data curation; formal analysis; investigation; methodology. **Haomiao Zhang**: Conceptualization; data curation; funding acquisition; investigation; methodology; resources; software; project administration; supervision; visualization; writing-original draft. **Jingdai Wang**: Conceptualization; project administration; supervision. **Yongrong Yang**: Conceptualization; project administration; supervision.

REFERENCES

1. E.Z.Velthoen M, M.Boereboom J, E.Bulo R, M.Weckhuysen B. Insights into the activation of silica-supported metallocene olefin polymerization catalysts by methylaluminoxane. *Catal. Today.* 2019;334:223-230.
2. Yuan S-F, Yan Y, Solan GA, Ma Y, Sun W-H. Recent advancements in N-ligated group 4

molecular catalysts for the (co)polymerization of ethylene. *Coordination Chemistry Reviews.* 2020;411.

3. Shoken D, Sharma M, Botoshansky M, Tamm M, Eisen MS. Mono(imidazolin-2-iminato) titanium complexes for ethylene polymerization at low amounts of methylaluminoxane. *J. Am. Chem. Soc.* 2013;135(34):12592-12595.
4. Tymińska N, Zurek E. DFT-D Investigation of Active and Dormant Methylaluminoxane (MAO) Species Grafted onto a Magnesium Dichloride Cluster: A Model Study of Supported MAO. *ACS Catal.* 2015;5(11):6989-6998.
5. Velthoen MEZ, Munoz-Murillo A, Bouhmadi A, Cecius M, Diefenbach S, Weckhuysen BM. The Multifaceted Role of Methylaluminoxane in Metallocene-Based Olefin Polymerization Catalysis. *Macromolecules.* 2018;51(2):343-355.
6. Glaser R, Sun X. Thermochemistry of the initial steps of methylaluminoxane formation. Aluminoxanes and cycloaluminoxanes by methane elimination from dimethylaluminum hydroxide and its dimeric aggregates. *J. Am. Chem. Soc.* 2011;133(34):13323-13336.
7. Bliemeister J, Hagendorf W, Harder A, et al. The Role of MAO-Activators. In: Fink G, Mülhaupt R, Brintzinger HH, eds. *Ziegler Catalysts: Recent Scientific Innovations and Technological Improvements*. Berlin, Heidelberg: Springer Berlin Heidelberg; 1995:57-82.
8. Kaminsky W. Discovery of Methylaluminoxane as Cocatalyst for Olefin Polymerization. *Macromolecules.* 2012;45(8):3289-3297.
9. Chien JCW, Wang B-P. Metallocene–methylaluminoxane catalysts for olefin polymerization. I. Trimethylaluminum as coactivator. *Journal of Polymer Science Part A: Polymer Chemistry.* 1988;26(11):3089-3102.
10. Reddy SS, Sivaram S. Homogeneous Metallocene-Methylaluminoxane Catalyst Systems for Ethylene Polymerization. *Progress in Polymer Science.* 1995;20(2):309-367.
11. Hoff R. *Handbook of Transition Metal Polymerization Catalysts*. John Wiley & Sons, Inc. 2018.
12. Kissin YV, Brandolini AJ. An Alternative Route to Methylalumoxane: Synthesis, Structure, and the Use of Model Methylalumoxanes as Cocatalysts for Transition Metal Complexes in Polymerization Reactions. *Macromolecules.* 2003;36(1):18–26.
13. Chen EY-X, Marks TJ. Cocatalysts for Metal-Catalyzed Olefin Polymerization: Activators, Activation Processes, and Structure−Activity Relationships. *Chem. Rev.* 2000;100:1391−1434.
14. Zijlstra HS, Joshi A, Linnolahti M, Collins S, McIndoe JS. Modifying methylalumoxane via alkyl exchange. *Dalton Trans.* 2018;47(48):17291-17298.
15. Tanaka R, Kawahara T, Shinto Y, Nakayama Y, Shiono T. An Alternative Method for the Preparation of Trialkylaluminum-Depleted Modified Methylaluminoxane (dMMAO). *Macromolecules.* 2017;50(15):5989-5993.
16. Bravaya NM, Panin AN, Faingol'd EE, et al. Isobutylalumoxanes as high-performance activators of rac-Et(2-MeInd)2ZrMe2 in copolymerization of ethylene with propylene and ternary copolymerization of ethylene, propylene, and 5-ethylidene-2-norbornene. *Polym. Bull.* 2015;73(2):473-491.
17. Pasynkiewicz S. Alumoxanes: Synthesis, structures, complexes and reactions. *Polyhedron.* 1990;9(2):429-453.
18. Bolesławski M, Serwatowski J. Investigations of the hydrolysis reaction mechanism of

organoaluminium compounds. 1H NMR spectroscopic studies on the R3Al/H2O reaction in polar solvents. *Journal of Organometallic Chemistry.* 1983;255(3):269-278.

19. Mason MR, Smith JM, Bott SG, Barron AR. Hydrolysis of tri-tert-butylaluminum: the first structural characterization of alkylalumoxanes [(R2Al)2O]n and (RAlO)n. *Journal of the American Chemical Society.* 1993;115(12):4971-4984.
20. Bravaya NM, Faingol'd EE, Babkina ON, et al. Syntheses of isobutylalumoxanes by triisobutylaluminum hydrolysis and their use as activators of dimethylated zirconocene in propylene polymerization. *Russ. Chem. Bull.* 2013;62:560–567.
21. Jensen KF. Flow chemistry-Microreaction technology comes of age. *AIChE Journal.* 2017;63(3):858-869.
22. Rogers L, Jensen KF. Continuous manufacturing – the Green Chemistry promise? *Green Chem.* 2019;21:3481-3498.
23. Hessel V, Kralisch D, Kockmann N, Noel T, Wang Q. Novel process windows for enabling, accelerating, and uplifting flow chemistry. *ChemSusChem.* 2013;6(5):746-789.
24. Bogdan AR, Dombrowski AW. Emerging Trends in Flow Chemistry and Applications to the Pharmaceutical Industry. *J Med Chem.* 2019;62(14):6422–6468.
25. Plutschack MB, Pieber B, Gilmore K, Seeberger PH. The Hitchhiker's Guide to Flow Chemistry. *Chemical Reviews.* 2017;117(18):11796-11893.
26. Sahoo HR, Kralj JG, Jensen KF. Multistep continuous-flow microchemical synthesis involving multiple reactions and separations. *Angew Chem Int Ed Engl.* 2007;46(30):5704-5708.
27. Adamo A, Beingessner RL, Behnam M, et al. On-demand continuous-flow production of pharmaceuticals in a compact, reconfigurable system. *Science.* 2016;352(6281):61-67.
28. Cole KP, Groh JM, Johnson MD, et al. Kilogram-scale prexasertib monolactate monohydrate synthesis under continuous-flow CGMP conditions. *Science.* 2017;356(6343):1144-1150.
29. Zhang H, Kopfmüller T, Achermann R, et al. Accessing multidimensional mixing via 3D printing and showerhead micromixer design. *AIChE Journal.* 2020;66(4):e16873.
30. Feng Y, Mu H, Liu X, et al. Leveraging 3D Printing for the Design of High-Performance Venturi Microbubble Generators. *Ind Eng Chem Res.* 2020;59(17):8447-8455.
31. Zentel KM, Fassbender M, Pauer W, Luinstra GA. Chapter Four - 3D printing as chemical reaction engineering booster. In: Moscatelli D, Sponchioni M, eds. *Advances in Chemical Engineering.* Vol 56: Academic Press; 2020:97-137.
32. Parra-Cabrera C, Achille C, Kuhn S, Ameloot R. 3D printing in chemical engineering and catalytic technology: structured catalysts, mixers and reactors. *Chem Soc Rev.* 2018;47(1):209-230.
33. Hou W, Bubliauskas A, Kitson PJ, et al. Automatic Generation of 3D-Printed Reactionware for Chemical Synthesis Digitization using ChemSCAD. *ACS Central Sci.* 2021;7:212–218.
34. Kitson PJ, Glatzel S, Chen W, Lin CG, Song YF, Cronin L. 3D printing of versatile reactionware for chemical synthesis. *Nat Protoc.* 2016;11(5):920-936.
35. Kitson PJ, Marie G, Francoia J-P, et al. Digitization of multistep organic synthesis in reactionware for on-demand pharmaceuticals. *Science.* 2018;359:aao3466.
36. Bird RB, Stewart WE, Lightfoot EN. *Transport Phenomena*. Wiley; 2006.
37. Thorn-Csányi E, Dehmel J, Dahlke B. Development of a method for the determination of the "free" trimethylaluminum content in methylalumoxane. *Macromol. Symp.* 1995;97:91-99.
38. Barron AR. New method for the determination of the trialkylaluminum content in alumoxanes.

Organometallics. 1995;14:3581-3583.